Iodine-131-MIBG Imaging to Monitor Chemotherapy Response in Advanced Neuroblastoma: Comparison with Laboratory Analysis

Simone Maurea, Secondo Lastoria, Corradina Caracò, Paolo Indolfi, Fiorina Casale, Maria T. di Tullio and Marco Salvatore

Nuclear Medicine Department, National Cancer Institute, CNR, University Federico II, and Pediatric Oncology, Second University of Medicine, Napoli, Italy

The rationale of this study was the evaluation of response to chemotherapy in children with advanced neuroblastoma using currently available diagnostic modalities. **Methods:** Iodine-131-metaiodobenzylguanidine (MIBG) imaging and 24-hr urinary vanillylmandelic acid (VMA) measurement were evaluated in 14 patients (7 males, 7 females, age range: 2–68 mo) with advanced neuroblastoma both pre- and postchemotherapy (5.6 ± 2.8 mo) as well as serum ferritin (FER) and neuron-specific enolase (NSE) levels in 9 and 8 patients, respectively. MIBG images were qualitatively compared in each patient. **Results:** Prechemotherapy, a total of 39 abnormal foci of MIBG uptake was detected. Postchemotherapy, 15 of these showed unchanged MIBG uptake, 7 had decreased uptake and 17 showed no uptake. In addition, four new abnormal foci of uptake were found. Postchemotherapy, a significant reduction of abnormal MIBG uptake ($p < 0.01$) was observed using a lesion-by-lesion analysis. When biochemical and MIBG postchemotherapy changes were compared, a significant relationship was found only between MIBG and VMA results ($r = 0.84$, $p < 0.01$). **Conclusions:** In postchemotherapy follow-up of children with advanced neuroblastoma, laboratory evaluation using VMA, FER and NSE measurements reflect only the global functional status of the disease, and are not helpful in defining the response of individual tumor lesions to treatment. Conversely, qualitative analysis using MIBG imaging may allow lesion-by-lesion evaluation of the heterogeneity of neuroblastoma response to chemotherapy. In this setting, changes in MIBG uptake are mirrored by the changes in catecholamine production, as measured by VMA levels.

Key Words: MIBG imaging; laboratory tests; neuroblastoma; chemotherapy

J Nucl Med 1994; 35:1429–1435

Neuroblastoma is one of the most common malignant neoplasms of early life (*1*). These tumors may be found wherever sympathetic nervous tissue is located, but they most often arise in the adrenal medulla or from the autonomic ganglia in the chest or abdomen. The malignant nature of these tumors consists of early metastases to lymph nodes, liver, bone marrow and skeleton. In children with advanced neuroblastoma, accurate tumor staging is necessary for treatment planning and for estimating the tumor prognosis (*1,2*). Surgery, radiation and/or chemotherapy are usually performed in different combinations in order to treat such patients (*1*). Particularly, in cases with metastases and/or an incompletely resected tumor, multiagent chemotherapy represents the appropriate treatment (*3*).

Although initial diagnostic work-up of advanced neuroblastoma is well established, the postchemotherapy follow-up evaluation is less well defined. Laboratory measurements have been proposed for monitoring tumor response to the treatment (*1*). In particular, urinary homovanillic and vanillylmandelic acids (VMA), serum ferritin (FER), neuron-specific enolase (NSE) and lactic dehydrogenase levels have been shown to increase in patients with actively growing neuroblastoma. However, these biochemical markers can only reflect the global active status of the total tumor masses, and they are not helpful in defining the response of individual lesions to the treatment. Computed tomography (CT) is the most accurate imaging modality to evaluate the postchemotherapy response of tumor lesions in advanced neuroblastoma (*3*). Metaiodobenzylguanidine (MIBG), a physiological analog of norepinephrine and guanethidine, has been shown to be taken up by neuroblastoma cells (*4*). This radiopharmaceutical, as a functional agent, is not taken up in fibrotic and/or necrotic tumor sites, but is taken up in viable neoplastic cells.

This study was undertaken to evaluate chemotherapy effects on individual tumor lesions in children with advanced neuroblastoma by monitoring MIBG uptake

Received Nov. 30, 1993; revision accepted Apr. 7, 1994.
For correspondence or reprints contact: Simone Maurea, MD, Via Raffaele De Cesare n. 7, 80132, Napoli, Italy.

TABLE 1
Clinical Data and Tumor Sites of the Patient Population and Corresponding Diagnostic Results

Patient no.	Age/Sex	Primary lesion/diagnostic tests	Other sites of disease/diagnostic tests
1	6 yr/F	Right adrenal/US	Liver/US, FNAB
2	5 mo/M	Mediastinum/x-ray, CT	Liver/US
3	5 yr/M	Mediastinum/x-ray, CT, MR	Liver/US
4	1 yr/M	Right adrenal/CT	Liver (micronodules)/CT
5	7 mo/F	Left adrenal/US, CT	Liver/US, CT
6	2 mo/M	Right paravertebral (D9-L3)/CT	Liver/FNAB
7	3 yr/M	Right adrenal/US, CT	Lymph nodes/US and bone/bone scan
8	3 yr/F	Mediastinum/x-ray, CT	Bone marrow/FNAB and bone/bone scan
9	1 yr/F	Abdominal/CT, MR	Bone marrow/FNAB and bone/bone scan
10	3 yr/F	Right adrenal/US, CT	Bone marrow/FNAB and bone/x-ray
11	4 yr/M	Mediastinum/x-ray, CT Left adrenal/CT	Lymph nodes/CT Bone marrow/FNAB
12	5 yr/M	Left adrenal/resected	Bone marrow/FNAB
13	5 yr/F	Left adrenal/resected	Lymph nodes/US and bone marrow/FNAB
14	3 yr/F	Pelvis/US, CT	Lymph nodes/CT Bone marrow/FNAB Bone/x-ray, CT, bone scan

US = ultrasound and FNAB = fine needle aspiration biopsy.

changes. MIBG findings were additionally compared to serial urinary VMA, serum FER and NSE measurements.

MATERIALS AND METHODS

Patient Population

Fourteen children (7 males and 7 females; age range 2–68 mo) with histologically proven advanced neuroblastoma (stage IV) were evaluated both before and after 5.6 ± 2.8 mo of chemotherapy (range 3–12 mo) using MIBG scintigraphy as well as 24-hr urinary VMA assay. Serial measurements of FER and NSE were also obtained in 9 and 8 patients, respectively. Table 1 illustrates the clinical data and the staging criteria for each patient. The chemotherapy regimen consisted of the AIEOP NB-82 protocol in one patient, AIEOP NB-85 protocol in eight patients and AIEOP NB-89 protocol in five patients (*5,6*). The AIEOP NB-82 protocol consisted of peptichemio, cisplatin and tenoposide for the induction phase (two cycles); cyclophosphamide, doxorubicin, peptichemio, cisplatin and tenoposide (one cycle) were used for the consolidation phase (*5*). The AIEOP NB-85 protocol consisted of peptichemio (one cycle), cyclophosphamide, vincristine and cisplatin (two cycles), as well as doxorubicin and tenoposide (one cycle) for the induction phase; similarly, peptichemio (one cycle), cyclophosphamide, vincristine and cisplatin (one cycle) as well as doxorubicin and tenoposide (one cycle) were used for the consolidation phase (*5*). The AIEOP NB-89 protocol consisted of peptichemio (two cycles), peptichemio and cisplatin (one cycle), cyclophosphamide, vincristine and cisplatin (two cycles), as well as doxorubicin and tenoposide (one cycle) for the induction phase; similarly, peptichemio (one cycle), cyclophosphamide, vincristine and cisplatin (one cycle), as well as doxorubicin and tenoposide (one cycle) were used for the consolidation phase (*6*).

Laboratory Measurements

The 24-hr urinary excretion rate of VMA was measured using spectrophotometric analysis, as previously described (*7*). Serum FER and NSE concentrations were determined by counterelectrophoresis using antibody to human FER and double-antibody radioimmunoassay, respectively (*8,9*).

MIBG Imaging

In all patients, both pre- and postchemotherapy radionuclide studies were performed using the same imaging protocols for data acquisition and processing. Medications which could potentially interfere with the tumor uptake of MIBG were discontinued for 30 days or longer before the study. Thyroid iodine uptake was previously blocked using a saturated solution of potassium iodide (12.5 mg per day orally begun 3 days before tracer administration and continued for 8 days). A dose of 0.1–0.5 mCi of ^{131}I-MIBG (Sorin Biomedica, Saluggia, Vercelli, Italy) was injected intravenously according to the body weight of each patient. Anterior and posterior spot images of the entire body were acquired in preset time (15 min/view) at 24, 48 and 72 hr after radiopharmaceutical administration with a large field-of-view gamma camera (GE Starport 400 Autotune, General Electric, Milwaukee, WI) equipped with a high-energy collimator and using a 128 × 128 matrix and a 20% window centered at the photopeak setting of 364 keV.

Data Analysis

MIBG images were considered abnormal when adrenal and/or extra-adrenal foci of increased uptake were seen on all 24, 48 and 72-hr scans. MIBG uptake was qualitatively graded using a five-point score: 0 = no visible uptake; 1 = barely visible uptake; 2 = clearly visible uptake; 3 = prominent uptake; and 4 = uptake yielding maximal film density, as previously described (*10*). To accurately evaluate post-treatment changes of MIBG uptake, pre- and postchemotherapy 48-hr images were directly evaluated in

TABLE 2
Pre- and Postchemotherapy Laboratory Measurement Results

Patient no.	Prechemotherapy			Postchemotherapy		
	VMA	FER	NSE	VMA (% change)	FER (% change)	NSE (% change)
1	5.7	1000	na	4.66	1000 (0) (=)	na
2	47	na	165.5	1 (98) (−)	na	12.2 (93) (−)
3	66	1322	65	4 (94) (−)	355 (73) (−)	6.5 (90) (−)
4	3.1	na	na	1.2	na	na
5	6	32.9	6.7	4.7	38.2	12.9
6	0.35	273	na	0.6	74	na
7	39.7	655	na	2.24 (92) (−)	712 (+9) (=)	na
8	4.9	1020	123	4.0	970.9 (−5) (=)	15.0 (90) (−)
9	40	na	na	40 (0) (=)	na	na
10	31.6	na	na	9 (72) (−)	na	na
11	141	na	46.9	29.5 (79) (−)	na	7 (85) (−)
12	18	1609	11.3	30 (40) (+)	2498 (55) (+)	19.1 (69) (+)
13	5	1700	38.8	6.8	512 (70) (−)	48.4 (24) (+)
14	5	467	95	20 (300) (+)	1458 (212) (+)	15.0 (84) (−)

VMA = urinary vanillylmandelic acid (normal values <11 mg/24 hr); FER = serum ferritin (normal values <300 ng/ml); NSE = serum neuron-specific enolase (normal values <15 μg/liter); na = not available; (=) indicates no level change; (−) indicates level decrease; (+) indicates level increase.

each patient. MIBG uptake scores, measured for each lesion on prechemotherapy images, were compared to the corresponding values obtained by the evaluation of postchemotherapy images. When an abnormal focus of MIBG uptake disappeared on postchemotherapy images, the score 0 was assigned to that lesion. The scores of the new lesions detected on postchemotherapy studies were not considered for the overall analysis. In all patients, bone scintigraphy was used to identify bony deposits of neuroblastoma, as previously described (*11*).

MIBG and laboratory data were then classified in terms of disease fate after chemotherapy. The criteria for MIBG results were established according to the changes in the grade of lesion uptake and/or evidence of new tumor sites. Disease regression consisted of disappearance and/or decrease of abnormal uptake (MIBG improvement). Disease progression consisted of the appearance of new abnormal foci of uptake (MIBG worsening). Stable disease consisted of no change in the number of tumor lesions as well as in abnormal uptake grading (MIBG no change).

Similarly, the criteria for laboratory results were established according to the presence of significant changes in the levels of each marker: disease regression = level decrease; disease progression = level increase; and stable disease = no level change. Level decrease consisted of a change from an abnormal to normal value or when a negative percent change between pre- and postchemotherapy values of at least 10% was observed. Level increase consisted of a change from a normal to abnormal value or when a positive percent change between pre- and postchemotherapy values of at least 10% was observed. No significant level change consisted of a percent change between pre- and postchemotherapy values less than 10%. When pre- and postchemotherapy laboratory results were in the normal range, biochemical data were not considered for comparison with MIBG changes.

Statistical Analysis

Data are expressed as mean ± 1 standard deviation. Differences in the mean values were assessed by Student's t-test for paired data. Relationships between MIBG changes and laboratory results after chemotherapy were assessed using the Spearman correlation test for ordinal data. Probability values <0.05 were considered significant.

RESULTS

Laboratory Measurements

Both pre- and postchemotherapy laboratory data for each patient are illustrated in Table 2. A postchemotherapy trend to lower levels of VMA and FER was observed. However, these differences were not statistically significant (VMA: 29 ± 38 prechemotherapy versus 11 ± 13 postchemotherapy; FER: 898 ± 585 prechemotherapy versus 846 ± 772 postchemotherapy). Conversely, a significant difference between pre- and postchemotherapy levels of NSE was found (69 ± 55 versus 17 ± 13, $p < 0.05$).

MIBG Imaging

The results of pre- and postchemotherapy MIBG studies for each patient are illustrated in Table 3. In particular, prechemotherapy a total of 39 neuroblastoma lesions with abnormal MIBG uptake were detected in all patients. Postchemotherapy, 17 tumor lesions showed no more MIBG uptake. Only 22 tumor lesions persisted: 15 had unchanged MIBG uptake and 7 showed decreased MIBG uptake. In addition, four new abnormal foci of MIBG uptake were localized. Figure 1 shows the results of the overall analysis of MIBG uptake in terms of mean values before and after the treatment. Postchemotherapy, an overall significant difference in MIBG uptake was observed ($p < 0.001$). Figure 2 shows an illustrative example regarding the heterogeneous response to chemotherapy in a patient (#14) with advanced neuroblastoma of MIBG imaging.

TABLE 3
Pre- and Postchemotherapy MIBG Imaging Results

Patient no.	Prechemotherapy		Postchemotherapy		MIBG result: disease fate
	Foci of MIBG uptake	Score	Foci of MIBG uptake	Score	
1	Right adrenal	3	Right adrenal	3	Worsening
	Liver	3	Liver	3	
			Bone (left pelvis) (new lesion)	2	
2	Superior mediastinum	3	Superior mediastinum	1	Improvement
	Liver	3	Liver	0	
3	Inferior mediastinum	1	Inferior mediastinum	0	Improvement
	Liver	2	Liver	0	
4	Right adrenal	3	Right adrenal	0	Improvement
5	Left adrenal	2	Left adrenal	0	Improvement
6	Right adrenal	2	Right adrenal	0	Improvement
7	Right adrenal	3	Right adrenal	3	Improvement
	Liver	2	Liver	0	
	Bone (right pelvis)	1	Bone (right pelvis)	0	
8	Superior mediastinum	3	Superior mediastinum	3	No change
	Bone marrow (spine and pelvis)	2	Bone marrow (spine and pelvis)	2	
	Right orbit	3	Right orbit	3	
	Bone marrow (right femur)	1	Bone marrow (right femur)	1	
	Bone marrow (left femur)	1	Bone marrow (left femur)	1	
9	Right adrenal	3	Right adrenal	3	Improvement
	Bone (skull)	3	Bone (skull)	1	
	Liver	3	Liver	0	
	Bone marrow (pelvis)	2	Bone marrow (pelvis)	0	
	Bone (right femur)	2	Bone (right femur)	0	
10	Right adrenal	3	Right adrenal	2	Improvement
	Bone marrow (skull)	3	Bone marrow (skull)	3	
	Bone marrow (pelvis)	2	Bone marrow (pelvis)	0	
11	Left superior mediastinum	1	Left superior mediastinum	0	Improvement
	Left adrenal	3	Left adrenal	3	
	Bone marrow (pelvis)	2	Bone marrow (pelvis)	0	
12	Bone marrow (pelvis)	1	Bone marrow (pelvis)	1	Worsening
	Bone marrow (sacrum)	2	Bone marrow (sacrum)	2	
	Bone marrow (right femur)	1	Bone marrow (right femur)	1	
			Bone marrow (spine) (new lesion)	2	
13	Bone marrow (pelvis)	2	Pelvis	0	Improvement
	Bone marrow (spine)	2	Bone marrow (spine)	0	
14	Left pelvis (para-vertebral)	3	Left pelvis (paravertebral)	2	Worsening
	Bone marrow (spine and pelvis)	3	Bone marrow (spine and pelvis)	1	
	Left femur	1	Left femur	0	
	Skull (parietal) (two foci)	2	Skull (parietal) (two foci)	1	
	Right orbit	3	Right orbit	3	
	Liver	2	Liver	1	
			Right abdomen (paravertebral) (new lesion)	3	
			Brain (occipital) (new lesion)	1	

Comparing MIBG and Biochemical Results

The direct comparisons between MIBG and VMA, as well as FER and NSE results in terms of disease fate, are illustrated in Table 4. The comparison between MIBG and VMA results was performed in eight patients. In seven of these patients (#2, 3, 7, 10–12, 14, 88%), the results of MIBG and urinary VMA were concordant (Table 4). The comparison between MIBG and FER, as well as NSE results, was performed in seven patients. In five of these patients (#3, 8, 12–14, 71%), the results of MIBG and serum FER were concordant (Table 4). In four patients (#2, 3, 11, 12, 57%), the results of MIBG and serum NSE were concordant (Table 4). A significant relationship was found only between MIBG and VMA changes after chemotherapy ($n = 8$, $r = 0.84$, $p < 0.01$).

DISCUSSION

In cancer, response to therapy consists of changes in tumor biology and ideally it should be assessed by histologic evaluation of tumor cell fibrosis and/or necrosis (*12*). In the postchemotherapy follow-up of children with advanced neuroblastoma, a precise diagnostic protocol should be used to evaluate the effects of the treatment on

Figure 1

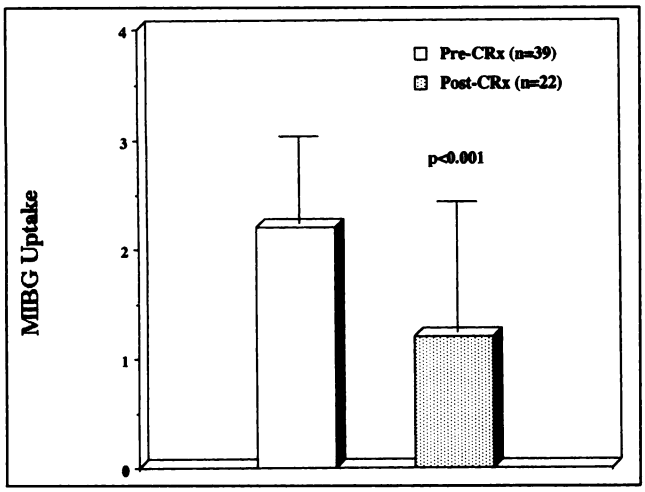

FIGURE 1. Pre- and postchemotherapy (CRx) mean values of MIBG uptake obtained by qualitative analysis in all patients (n = no. of lesions analyzed).

TABLE 4
Direct Comparisons Between MIBG and Laboratory Results in Terms of Regression, Progression and Stable Disease after Chemotherapy

	Decrease	Increase	No Change
VMA levels (n = 8)			
MIBG improvement	5	0	1
MIBG worsening	0	2	0
MIBG no change	0	0	0
FER levels (n = 7)			
MIBG improvement	2	0	1
MIBG worsening	0	2	1
MIBG no change	0	0	1
NSE levels (n = 7)			
MIBG improvement	3	1	0
MIBG worsening	1	1	0
MIBG no change	1	0	0

both primary and metastatic tumor sites. To assess the patient global performance status, clinical and physical examinations should always be performed. Different serum and urinary laboratory measurements have been suggested as useful markers of tumor activity (*3*). However, these biochemical tests reflect only the integrated biofunctional status of the total tumor masses and they are not helpful in accurately defining the response of individual tumor lesions to the treatment. To evaluate the lesion-by-lesion response to chemotherapy in advanced neuroblastoma, imaging studies are usually performed (*1–3*).

Post-treatment size changes of tumor sites can be measured with CT and/or other diagnostic imaging modalities and represent the basic criterion to assess chemotherapy effects using these techniques (*1–3*). However, this approach does not provide information about the nature of the detected lesions which may contain only fibrotic and/or necrotic nonviable tissue (*13*). This is usually not crucial in the initial work-up and staging of such patients since diagnosis is made by biopsy. Conversely, the differentiation of viable tissue from fibrosis and/or necrosis within the remnant tumor is fundamental in evaluating chemotherapy effects.

Radionuclide imaging is widely used to evaluate cancer. Although nuclear medicine studies do not provide specific anatomic details of neoplastic lesions, these techniques have been shown to be powerful tools for monitoring tumor response in patients undergoing chemotherapy and/or radiotherapy (*14*). The analysis of tumor activity can be used as functional marker since uptake of labeled compounds reflects cellular and/or other physiologic functions in neoplastic tissues. In particular, MIBG has been shown to be concentrated into the neurosecretory granules of normal and neoplastic chromaffin tissue such as neuroblastoma (*4*). In this setting, this radiopharmaceutical, as a functional agent, is not taken up in fibrotic and/or necrotic tissues, but only in viable neoplastic cells. Therefore, this radionuclide imaging technique shows reasonable features

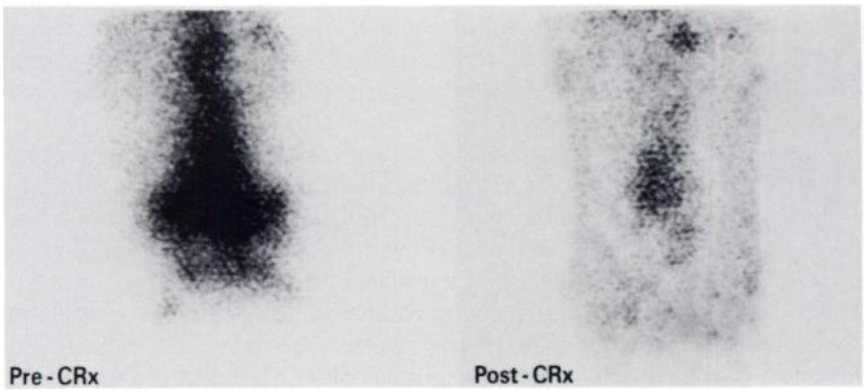

FIGURE 2. Forty-eight hour MIBG images of Patient 14 with prechemotherapy (Pre-CRx) on the left and postchemotherapy (Post-CRx) on the right. Posterior view of the abdomen and pelvis: on prechemotherapy image, abnormal MIBG uptake is present in the spine, pelvis, liver and left femur; the abnormal MIBG uptake of the mass detected in the left pelvis by US and CT is obscured from the other foci of uptake; on postchemotherapy image, the intensity of MIBG uptake in the spine, pelvis and liver is clearly reduced; the lesion in the left femur is not detectable. Abnormal but decreased uptake is still present in the right pelvis and the mass detected on US and CT is now clearly visible; however, this last lesion had no size changes on US and CT. A new focus of abnormal MIBG uptake is seen in the right upper abdomen in paravertebral location.

to monitor tumor response to different forms of therapy in advanced neuroblastoma (*14*).

Recently, Englaro et al. (*15*) used ^{131}I-MIBG imaging in children undergoing bone marrow transplantation for neuroblastoma. These authors suggested that this imaging technique is very specific and valuable in evaluating such patients before and after this type of treatment. In particular, the same acquisition and processing parameters have to be used to evaluate chemotherapy effects in cancer patients using scintigraphic images. The need for this is to accurately assess the degree of changes in tracer uptake on images acquired at different times.

In this study, we reported our experience in evaluating tumor response to chemotherapy in children with advanced neuroblastoma comparing ^{131}I-MIBG imaging and VMA, FER and NSE laboratory results. Our data demonstrated that, while biochemical measurements provide only a global evaluation of the disease fate and no information regarding the response of each tumor lesion to the treatment, MIBG imaging allows lesion-by-lesion evaluation of tumor response by measuring changes in tracer uptake. Thus, it may be suggested as a marker to monitor chemotherapeutic effects. However, in this study, three patients (#4–6) did not show evidence of abnormal MIBG uptake in metastatic liver lesions. This finding is not surprising since MIBG is physiologically concentrated in the liver and, therefore, small lesions can be obscured. In these cases, MIBG results should be integrated for better evaluation using other imaging studies.

In our series, in three patients in whom the overall laboratory and MIBG results were concordant in terms of disease regression, one lesion for each patient persisted on scintigraphic images; one with reduced uptake (#2) and two with unchanged uptake (#7 and #11). On the other hand, in two patients (#12 and 14) in whom the overall laboratory and MIBG results were concordant in terms of disease progression, new lesions were detected by radionuclide images. In particular, Patient 14 is an illustrative example of the heterogeneity of neuroblastoma response to chemotherapy. In this patient, five abnormal foci of MIBG uptake were localized on prechemotherapy study. Posttreatment, four of these lesions had decreased MIBG uptake and one lesion located in the left femur disappeared; in addition, two new abnormal foci of MIBG uptake were detected in the superior right abdominal area and in the occipital region of the skull, respectively.

The heterogeneity of neuroblastoma response to chemotherapy, as shown in this study by means of MIBG results, may have important clinical implications, particularly when alternative therapeutic approaches are contemplated and/or prognostic observations are requested. When postchemotherapy MIBG findings were further compared in all cases with long-life follow-up, concordant results were found in 9 (64%) of the 14 children: MIBG improvement associated with complete disease remission (n = 5, #2–6); MIBG worsening associated with patient death (n = 3, #1, 12, 14); and no MIBG change associated with successive disease progression (n = 1, #8). Conversely, discrepancies in 5 (36%) of the 14 children were observed. In these 5 patients, although MIBG improvement was found on postchemotherapy images, a poor outcome occurred later on with disease progression and patients' death in 2 (#9 and 11) and 3 (#7, 10, 13) patients, respectively. In these latter children, postchemotherapy MIBG improvement could reflect only successful, but temporary, response to the treatment and skeletal involvement since disease presentation could explain the disease fate. Therefore, the definite outcome in the whole group of children was more strictly related, in the majority of cases (13/14), to the disease extent at initial presentation on MIBG imaging rather than to MIBG postchemotherapy results. In particular, a complete and persistent disease remission was obtained in 5 of the 6 children presenting only soft-tissue metastases (i.e., liver, lymph nodes, etc.) since initial presentation.

In this report, when laboratory and MIBG postchemotherapy results were directly compared, a significant relationship between changes in MIBG uptake and VMA levels was observed. This finding is concordant with a previous study in which MIBG uptake and VMA level changes were compared in patients with malignant pheochromocytoma treated with chemotherapy (*16*). These results are reasonable because MIBG is an analog of catecholamines and VMA is one of their metabolites. As expected, the lack of correlations between MIBG uptake and FER, as well as NSE level changes after chemotherapy found in this study, is not surprising because these two tumor markers are not related to catecholamine metabolism. Therefore, these data suggest that changes in MIBG uptake after chemotherapy are mirrored by changes in catecholamine production, as measured by VMA levels. Furthermore, our results are also in agreement with previous studies in which MIBG and laboratory tests were used in the postchemotherapy follow-up of children with advanced neuroblastoma (*17,18*).

In our series, the direct comparison between biochemical and MIBG changes was not performed in all patients because biochemical levels occurred in the normal range in a few patients either pre- or postchemotherapy. This finding deserves some comments. In fact, in these patients, biochemical markers failed to recognize the presence of neuroblastoma. This result is concordant with our previous data obtained in a larger series of 40 neuroblastoma patients in which the diagnostic accuracy of MIBG imaging was significantly higher than VMA, FER and NSE measurements (*19*).

In conclusion, in the postchemotherapy follow-up of children with advanced neuroblastoma, laboratory measurements including VMA, FER and NSE reflect only the global functional status of the disease, but are not helpful in defining the response of individual tumor lesions to the treatment. Conversely, qualitative analysis using MIBG imaging allows lesion-by-lesion evaluation of the heterogeneity of neuroblastoma response to chemotherapy. In this setting, changes in

MIBG uptake are mirrored by the changes in catecholamine production as measured by VMA levels.

REFERENCES

1. Vaorhess ML. Disorders of the adrenal medulla and multiple endocrine adenomatosis syndromes. In: Solomon A, *Clinical pediatric endocrinology*. Philadelphia: W.B. Saunders 1990:235–258.
2. Bousvaros A, Kirks DR, Grossman H. Imaging of neuroblastoma: an overview. *Pediatr Radiol* 1986;16:89–106.
3. Brodeur GM, Seeger RC, Barrett A, et al. International criteria for diagnosis, staging and response to treatment in patients with neuroblastoma. *J Clin Oncol* 1988;6:1874–1881.
4. Shapiro B, Gross MD. Radiochemistry, biochemistry and kinetics of ^{131}I-metaiodobenzylguanidine (MIBG) and ^{123}I-MIBG: clinical implications of the use of ^{123}I-MIBG. *Med Ped Oncol* 1987;15:170–177.
5. De Bernardi B, Carli M, Casale F, et al. Standard-dose and high-dose peptichemio and cisplatin in children with disseminated poor-risk neuroblastoma: two studies by the Italian cooperative group for neuroblastoma. *J Clin Oncol* 1992;10:1870–1878.
6. Garaventa A, Conte M, Paolucci P, et al. Neuroblastoma disseminato. Risultati preliminari del protocollo AIEOP NB-89 [Abstract]. Atti del XX Congresso Nazionale A.I.E.O.P., Bari, Italy; 1993:207.
7. Pisano JJ, Crout JR, Abraham D. Determination of 3-methoxy-4-hydroxymandelic acid in urine. *Clin Chim Acta* 1962;7:285–291.
8. Hann H-WL, Levy HM, Evans AE. Serum ferritin as a guide to therapy in neuroblastoma. *Cancer Res* 1980;40:1411–1413.
9. Zeltzer PM, Marangos PJ, Parma AM, et al. Raised neuron-specific enolase in serum of children with metastatic neuroblastoma. *Lancet* 1983;2:361–363.
10. Nakajo M, Shapiro B, Copp J, et al. The normal and abnormal distribution of the adrenomedullary imaging agent m-(I-131)iodobenzylguanidine (^{131}I-MIBG) in man: evaluation by scintigraphy. *J Nucl Med* 1983; 24:672–682.
11. Lastoria S, Maurea S, Caracò C, et al. Iodine-131-metaiodiobenzylguanidine scintigraphy for localization of lesions in children with neuroblastoma: comparison with computed tomography and ultrasonography. *Eur J Nucl Med* 1993;20:1161–1167.
12. Miller AB, Hoogstraten B, Staquet M, Winkler A. Reporting results of cancer treatment. *Cancer* 1981;47:207–214.
13. Lewis E, Bernardino ME, Salvador PG, et al. Post-therapy CT-detected mass in lymphoma patients: is it viable tissue? *JCAT* 1982;6:792–795.
14. Front D, Israel O. Nuclear medicine in monitoring response to cancer treatment. *J Nucl Med* 1989;30:1731–1736.
15. Englaro EE, Gelfand MJ, Harris RE, Smith HS. Iodine-131-MIBG imaging after bone marrow transplantation for neuroblastoma. *Radiology* 1992;182: 515–520.
16. Maurea S, Reynolds JC, Cuocolo A, Keiser HR, Neumann RD. Iodine-131-MIBG scintigraphy for monitoring response to chemotherapy in malignant pheochromocytoma: comparison with urinary biochemical analysis [Abstract]. *J Nucl Med* 1991;32:1044.
17. Ikekubo K, Habuchi Y, Jeong S, et al. A follow-up study using iodine-131-metaiodobenzylguanidine imaging in a patient with neuroblastoma. *Clin Nucl Med* 1986;11:777–780.
18. Yeh SD, Helson L, Benua RS. Correlation between iodine-131-MIBG imaging and biological markers in advanced neuroblastoma. *Clin Nucl Med* 1988;13:46–52.
19. Lastoria S, Maurea S, Caracò C, et al. Pitfalls in the diagnosis of neuroblastoma: a comparative study using iodine-131-MIBG scintigraphy and laboratory measurements [Abstract]. *J Nucl Med* 1992;33:930.